

AI in Electrocardiology

O 1. ECG-based unsupervised clustering in coronary artery disease associates with cardiovascular events

Josseline Madrid¹, Patricia Munroe², Stefan Duijvenboden³, Ana Mincholé¹, Julia Ramírez¹

¹ Universidad de Zaragoza, Spain, ² Queen Mary University of London, UK, ³ University of Oxford, UK

Background: Coronary artery disease (CAD) is a leading cause of mortality worldwide. It slows ventricular conduction and increases dispersion of repolarization, manifesting differently on the electrocardiogram (ECG). We hypothesize there are distinct ECG morphological phenotypes in CAD that specifically associate with cardiovascular risk events.

Objective: This study aimed to identify distinct clusters of CAD individuals based on ECG morphological phenotypes using unsupervised learning. Moreover, to investigate the association of belonging to each cluster with risk of atrial fibrillation (AF), heart failure (HF) and ventricular arrhythmias (VA).

Methods: We calculated the median heartbeat ECG from 15-second ECGs (lead I) from participants in the UK Biobank imaging study with prevalent CAD (N = 1,198). Standard and morphology-based indices were extracted and fed into an unsupervised clustering model to identify two distinct clusters. We then allocated these clusters to participants from an independent cohort from UK Biobank with CAD and ECG data (N = 1,109). We tested the association of each cluster with prevalent AF, HF or VA risk.

Results: Individuals in cluster 1 exhibited reduced ventricular conduction and increased repolarization dispersion, including 10 ms wider QRS and 25 ms longer QT intervals on average, compared to individuals in cluster 2 (Figure). These differences were independent from age, gender and other clinical risk factors. Subjects in cluster 1 had a higher rate of HF events in prevalent (9.7%, $p < 0.001$) association analysis.

Conclusions: Our analysis identified different groups of CAD subjects, each with similar ECG characteristics, with important implications on risk detection, offering affordable and fast risk assessment.

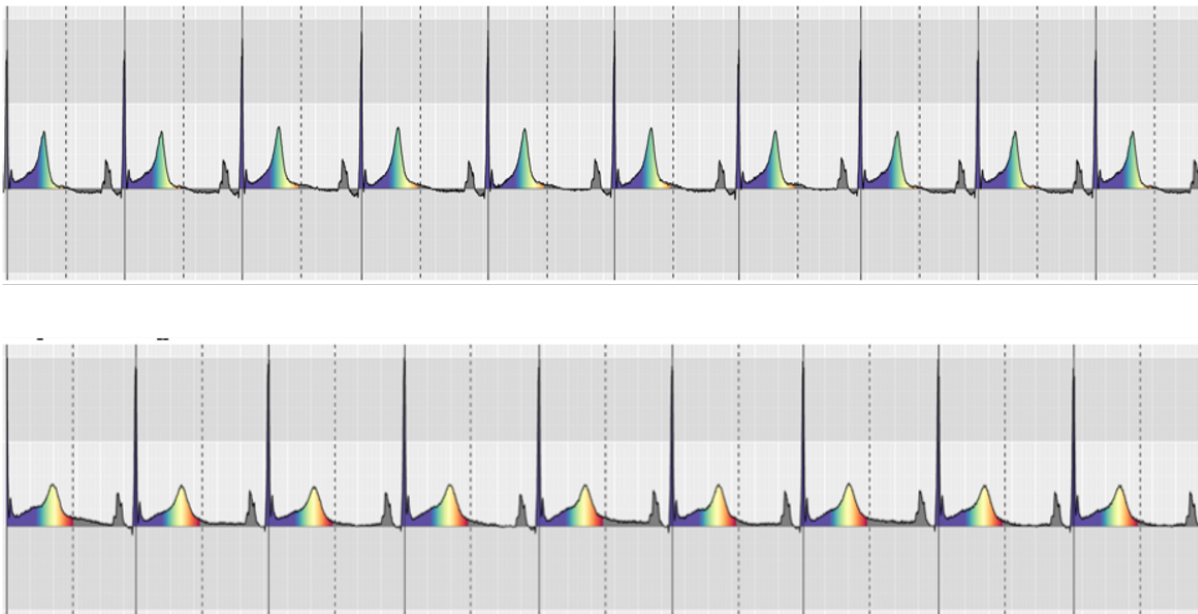
O 2. Attitudes of clinicians to a ‘human-like’ explainable AI based on pseudo-colouring of ECGs that exposes life-threatening anomalies

Lukas Hughes-Noehrer^{1,2}, Alaa Alahmadi¹, Leda Channer¹, Adina Rahim¹, Richard Body^{1,2}, Caroline Jay¹

¹ The University of Manchester, UK, ² Manchester University NHS Foundation Trust, UK

AI and machine learning technologies are changing how we study and interpret electrocardiograms (ECG). To ensure they are fit for purpose, it is important that their development is closely aligned with the priorities of those making clinical decisions and patients receiving care, from the earliest stages. In this study, we investigate clinicians’ attitudes towards AI technologies and in particular the potential of a novel approach of pseudo-colouring ECGs to expose life-threatening changes (QT-prolongation and STEMI), which show how an automated, explainable, algorithm is working. We conducted a series of interviews with junior doctors and clinicians from five specialties (emergency medicine, anaesthesia and critical care, cardiology, primary care, and paramedics) in the UK, spanning all career stages. Our study: (i) documents their approach to computational ECG interpretation, (ii) explores the potential of our novel pseudo-colouring approach (representing abnormal changes in signal duration/amplitude using a sequence of colours) and other future ‘human-like’ computing approaches to facilitate ECG interpretation and support clinical decision making, and (iii) elicits their opinions about the importance of explainability and trustworthiness of AI algorithms. The results of our study show that clinicians have an overwhelmingly positive attitude toward digitally enhanced and AI supported ECGs and our pseudo-colouring visualisation approach is their preferred method of presentation, when compared with other contemporary approaches, such as fully automated read-outs and ECG measurements. Based on our preliminary work and the stakeholder engagement study, ECG technology based on AI-driven human-like computing applications seems to be a promising way both to facilitate interpretation of ECGs, and to highlight difficult to spot or overlooked pathologies, helping to make ECGs easier to understand for clinicians and laypeople alike.

Figure 1: Novel algorithm to pseudo-colour QT interval. Upper row: patient with normal QT interval. Bottom row: patient with QT prolongation. Both strips at HR 60 BPM.



O 3. Deep learning model-enabled electrocardiogram to localize premature ventricular contractions in patients referred for catheter ablation

Abhishek Deshmukh¹, Tiffany Woelber¹

¹Mayo Clinic, Rochester, MN, USA

Introduction: Accurate pre-procedure localization of the premature ventricular contractions (PVCs) is critical in preparing for the ablation. So far, no tools exist for artificial intelligence guided PVC-localization.

Hypothesis: Trained deep learning model will be able to predict the site of origin (SOO) of PVCs using 12 lead ECG.

Methods: We analyzed 707 ECG-ablation pairs from 2403 patients who had at least one ECG flagged for PVCs in the 6 months prior to their procedure. First, we used a cohort of 100,000 ECGs without PVCs and 10,000 ECGs with PVCs to train a convolutional neural network (CNN) to isolate the ECG segments with PVCs in them from a 12-lead ECG (Figure 1). We then trained two models, one utilizing a 10-second 12-lead ECG, and the other with just the isolated PVC beats as input. The models were trained using the Keras framework with TensorFlow (Google).

Results: The mean age of the patients in the cohort was 61.2 ± 15.0 years. 66.3 percent of patients underwent left ventricle ablation, 54.6 percent had outflow ablation, and 55.3 percent had ablation of sites with leftward axis (septal location for midline and left ventricle PVCs). The model trained on 10-second ECGs yielded validation and test AUCs of 0.941 and 0.931 for outflow, 0.898 and 0.891 for ventricle, and 0.863 and 0.846 for leftward axis (Figure 1A). The model trained on isolated segments containing PVC beats yielded validation and test AUCs of 0.966 and 0.957 for outflow, 0.879 and 0.907 for ventricle, and 0.846 and 0.829 for SOO for leftward axis (Figure 1B).

Conclusions: We have trained an accurate convolutional neural network that can predict SOO using the surface ECG. Further fine-tuning would be needed to refine the model and develop prediction of specific sites.

Electrocardiology in Cardiogenetic disease

O 4. Electrocardiographic phenotype as quantified by ECG Risk-score has higher predictive power than HCMRisk-Kids, PRIMACY and ESC HCM risk-calculators in childhood hypertrophic cardiomyopathy

Ingegerd Östman-Smith^{1,2}, Gunnar Sjöberg³, Eszter Szepesvary⁴, Jenny Alenius Dahlqvist⁵, Per Larsson⁶, Eva Fernlund⁷

¹ Institute Of Clinical Specialties, Sahlgrenska Academy, Gothenburg University, ² Childrens Heart Center, Queen Silvia Childrens Hospital, Gothenburg, Sweden, ³ Department of Women's and Children's Health, Karolinska Institute, Stockholm, Sweden, ⁴ Department of Paediatrics, John Radcliffe Hospital, Oxford United Hospital Trust, Oxford, UK, ⁵ Department of Clinical Sciences, Umeå University, Umeå, Sweden, ⁶ Department of Pediatric Cardiology, Uppsala University, Children's Hospital, Uppsala, Sweden, ⁷ Department of Clinical and Experimental Medicine, Linköping University, Division of Pediatrics, Crown Princess Victoria Children's Hospital, Linköping University Hospital, Linköping, Sweden

Introduction: Hypertrophic cardiomyopathy (HCM) is the commonest cause of medical sudden death in children. Existing risk-calculators use symptoms and morphological features to predict risk of sudden cardiac death (SCD). The ECG phenotype as characterized in the ECG risk-score has shown promise in both childhood- and adult HCM.

Purpose: To compare the predictive power of the ECG Risk-score with other risk-calculators.

Methods: 203 HCM-patients, 65% male, diagnosed ≤ 19 years of age, were identified in Swedish and English cohorts. Median age at diagnosis was 11.3 years. The end-point was sudden death, cardiac arrest or appropriate ICD-discharge (SCD/CA); mean follow-up was 13.9 years. ECG Risk-score was calculated according to doi:10.1093/eurheartj/ehp443, and PRIMACY, HCMRisk-Kids and ESC HCM-Risk-SCD scores using web-based calculators.

Results: During follow-up 40 SCD/CA occurred at a median age of 17 years. On univariate Cox-hazard regression analysis both ECG Risk-score, HCMRisk-Kids score, PRIMACY score, and after 16 years of age ESC HCM Risk-SCD score (n=155) were significant risk-factors for SCD/CA (all $p < 0.001$). In Cox-hazard analysis ECG Risk-score remained highly significant ($p < 0.001$) paired with HCMRisk-Kids ($p = 0.044$) and PRIMACY ($p = 0.037$). For > 16 years old: ESC Risk-score ($p = 0.028$) is independent of ESC HCM Risk-SCD ($p = 0.023$). ECG Risk-scores in patients with SCD/CA within 5 years of diagnosis were 9 [7-10] versus 3 [1-4] in patients without events. Comparing power to predict SCD/CA within 5 years, respective ROC-curves have following C-statistic: ECG Risk-score > 5 at diagnosis: 0.87 [0.79-0.94], sensitivity 94%, $p < 0.001$; HCM Risk-Kids ≥ 6 : 0.74 [0.62-0.86], sensitivity 78%, $p = 0.001$; PRIMACY ≥ 9 : 0.71 [0.58-0.84], sensitivity 72%, $p = 0.004$. For > 16 years: ECG risk-score ≥ 16 : 0.81 [0.70-0.91], $p < 0.001$ and ESC HCM Risk-SCD ≥ 6 : 0.79 [0.63-0.96], sensitivity 75%, $p = 0.001$.

Conclusions: The ECG Risk-score is a risk-factor independent of alternative risk-algorithms and has highest predictive power and sensitivity.

O 5. Electrical repolarization pathway by CineECG characteristics in LQTS

Ksenia Sedova¹, Peter Van Dam², Pia Dahlberg³, Anneli Svensson⁴, Pyotr G. Platonov⁵

¹ Department of Biomedical Technology, Faculty of Biomedical Engineering, Czech Technical University in Prague, Kladno, Czech Republic, ²Center for Digital Medicine and Robotics, Jagiellonian University Medical College, Krakow, Poland, ³ Department of Cardiology, Department of Molecular and Clinical Medicine, Institute of Medicine, Sahlgrenska Academy, Gothenburg, Sweden, ⁴ Department of Cardiology and Department of Health, Medicine and Caring Sciences, Linköping University, Linköping, Sweden, ⁵ Department of Cardiology, Institution for Clinical Sciences, Lund University, Lund, Sweden

Background: In patients with long QT syndrome (LQTS), abnormal repolarization expressed in QTc duration and T-wave morphology changes dynamically, which is associated with the risk of arrhythmias. CineECG visualization technique allows to assess the spatial heterogeneity and could be helpful for the detection of electro-anatomical markers of abnormal repolarization to support early diagnosis and risk assessment in LQTS.

Objective: To evaluate CineECG-derived repolarization path directions and to test them for the association with the QT interval prolongation in LQT1 and LQT2 patients.

Methods: In total, 103 LQTS patients had median QTcB 465 [445;482] ms at initial presentation (63 LQT1 and 40 LQT2). 12-lead ECGs were retrieved from digital ECG archive and processed using CineECG, which computes the average electrical pathway in a generic heart/torso model. Repolarization path directions were computed for STT interval and compared between the maximal QTc ECG (maxQTc ECG) and baseline ECG. Repolarization path directions have values between -1 (total congruence) and +1 (an opposite direction) regarding posterior-anterior, right-to-left, and apicobasal heart axes.

Results: At baseline, STT path directions showed predominantly apicobasal repolarization sequence and did not differ between LQT1 and LQT2. QTc prolongation was associated with the STT path direction change on the apicobasal axis in LQT1 (-0.91 vs -0.88, $p=0.001$; maxQTcB 502 [487;536] ms) and on the right-to-left axis in LQT2 (-0.15 vs -0.11, $p=0.049$; maxQTcB 521 [488;577]). In LQT1, the baseline apicobasal repolarization gradient was associated with maxQTc ($B=55.31$, $p=0.002$). In LQT2 patients, no associations between repolarization path directions at baseline and maxQTc were observed.

Conclusion: In patients with LQTS, QTc prolongation during follow-up was associated with the genotype-dependent change of the direction of the average repolarization path, detectable with CineECG. Cine-ECG-derived apicobasal repolarization direction at baseline ECG was linearly related to the degree of QTc prolongation during follow-up in LQT1 patients.

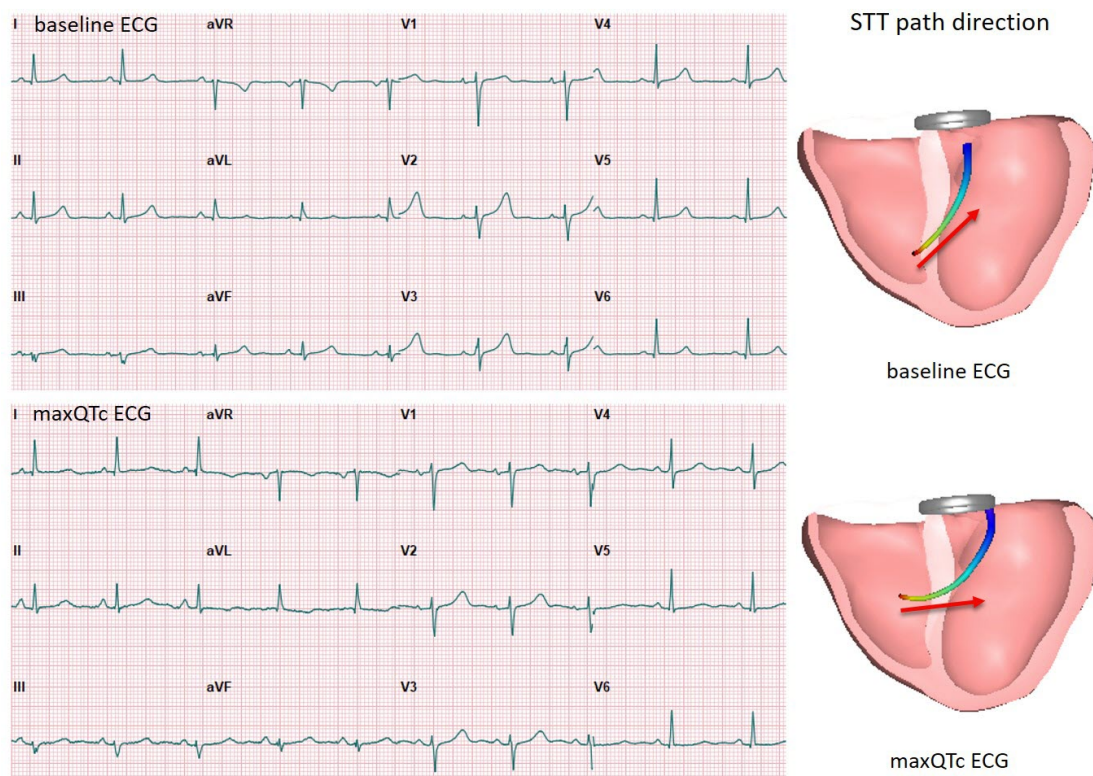


Figure: Representative 12-lead ECGs and apicobasal repolarization path direction for baseline and maxQTc ECGs in LQT1 patient.

O 6. Longitudinal analysis of 10-second-long ECG-derived biomarkers from patients suffering Brugada Syndrome

Alba Isabel-Roquero¹, Monica Veenhoven², Pedro Gomis², Flavio Palmieri³, Elena Arbelo^{4,5}

¹ Institut d' Investigació August Pi y Sunyer (IDIBAPS), Barcelona, Spain, ² ESAII Department, EEBE, CREB, Universitat Politècnica de Catalunya, Barcelona, Spain, ³ Biophysics unit, Department of Physiological Sciences, Faculty of Medicine and Health, Universitat Barcelona, Bellvitge Campus, Barcelona, Spain, ⁴ Arrhythmias section, Hospital Clínic, Barcelona, Spain, ⁵ European Reference Network for rare, low prevalence complex diseases of the heart - ERN GUARD-Heart

Brugada syndrome (BrS) is a rare inherited cardiovascular channelopathy predisposing to ventricular arrhythmias (VA) and sudden cardiac death (SCD) which is normally diagnosed by *a posteriori* cardiac events, such as the presence of resuscitated cardiac arrest or arrhythmogenic syncope. The electrocardiogram (ECG) is a well-established diagnostic tool and it is known that BrS is associated with specific ECG patterns, most of them related to the QT interval, which could be used for risk stratification. However, their clinical value is yet to be fully investigated.

In this work, we aim to assess the risk stratification performance of 11 ECG-derived biomarkers based on the QT interval. For this purpose, we performed a 6-year-long longitudinal analysis of 10-second-long ambulatory ECGs from 38 patients suffering BrS. The BrS lead configuration, obtained by placing the electrodes in the high precordial lead disposition (up to the second intercostal space above normal), was adopted.

Each ECG was preprocessed, including noise and artifact removal, and the start, peak, and end positions of each wave in every heartbeat were found. Then, the ST deviation at J-point and J-point + 60 ms, ST slope, QT interval, corrected QT interval, average power of QRS, absolute value of QRS area, T wave symmetry, T duration, T peak and symmetry of the ST-T-wave complex were computed, and their time evolution trend was evaluated for each patient. Preliminary results showed a considerable increase in the median value of the proposed biomarkers, especially in the precordial leads, over the years, confirming their ability to increase the sensitivity of the ECG for detecting the BrS. Nonetheless, further analysis over a larger population, also including a control group, is needed to confirm these findings and validate their diagnostic power.

O 7. Assessing seroprevalence to adeno-associated virus serotype 9 (AAV9) in preparation for RIDGE™-1, a phase 1b first-in-human study to evaluate safety and efficacy of TN-401 investigational gene therapy in adults with PKP2-associated arrhythmogenic right ventricular cardiomyopathy (ARVC)

Natalia Paterson¹, Hugh Calkins², Vasanth Vedentham³, Neal K Lakdawala⁴, Wilson Tang Wai Hong⁵, John R Giudicessi⁶, Matthew RG Taylor⁷, Antonis Pantazis⁸, Larry A Chinitz⁹, Perry Mark Elliott¹⁰, Phillippe Chevalier¹¹, Jeff Haroldson¹, Whedy Wang¹, Gretchen Argast¹, Whit Tingely¹, Matt Pollman¹

¹ Tenaya Therapeutics, San Francisco, USA, ² John Hopkins University, Baltimore, USA, ³ University of California, San Francisco, USA, ⁴ Brigham and Women's Hospital, Boston, USA, ⁵ Cleveland Clinic, Ohio, USA, ⁶ Mayo Clinic Rochester, USA, ⁷ University of Colorado Hospital, Colorado, USA, ⁸ Royal Brompton, London, UK, ⁹ NYU Langone Health, New York, USA, ¹⁰ University College London, London, UK, ¹¹ Academic Hospital of Lyon, France

Background: ARVC is a severe disease with sudden cardiac death as the initial presentation in nearly 25% of patients. PKP2 mutations are the genetic cause in ~40% of ARVC cases. Current management of ARVC relies on palliative therapies that fail to alter disease course. Tenaya Therapeutics has developed TN-401, an investigational AAV9-based gene therapy designed to restore the expression and function of PKP2 gene in the heart. AAV9 is the most studied capsid with clinical validation in human hearts. Preclinical evidence in PKP2 knock-out mouse models supports TN-401 as a potential gene therapy approach being explored in RIDGE-1, a Phase 1b clinical trial (NCT:06228924) currently enrolling symptomatic adults with PKP2 mutations.

Purpose: Neutralizing antibodies to AAV9 capsids obtained through previous exposure to naturally occurring, wild-type virus might compromise the efficacy and safety of TN-401 by eliciting an immune response, making it important to assess antibody status prior to enrollment in the RIDGE-1 study. The RIDGE non-interventional natural history and seroprevalence study (NCT:06311708) is underway to characterize PKP2-associated ARVC and to assess preexisting antibody titers in patients who may be eligible for the RIDGE-1 study.

Methods: We analyzed interim seroprevalence results from 54 patients at 9 centers participating in the RIDGE study, generated using a single, blood-based laboratory test.

Results: Based on this interim analysis, the majority (80%) of participants tested to date with PKP2-associated ARVC would be eligible for the RIDGE-1 study, with no differences across age, gender or geographic region.

Conclusions: The RIDGE-1 interventional study is exploring gene therapy to address the underlying genetic cause of disease in PKP2-associated ARVC patients. Interim analysis of AAV9 neutralizing antibody titer illustrate most patients may be eligible to participate in RIDGE-1. Genetic testing for ARVC patients to identify pathogenic mutations including PKP2 is important as they may be eligible to participate in RIDGE-1.

Table 1. Baseline Characteristics: 54 Patients Enrolled Between APR2023 and MAR2024

Baseline Characteristics	Summary Statistics
Age	
N	54
Mean (SD)	42.4 (13.92)
Min – Max	21 – 64
Sex	
Female % (n/N)	39% (21/54)
Male % (n/N)	61% (33/54)
Race	
Asian % (n/N)	4% (2/54)
Black % (n/N)	4% (2/54)
White % (n/N)	93% (50/54)
Ethnicity	
Not Hispanic or Latino % (n/N)	100% (54/54)
PKP2 Variant	100%
Pathogenic % (n/N)	93% (50/54)
Likely pathogenic % (n/N)	22% (12/54)
NYHA Class	
I	65% (35/54)
II	30% (16/54)
III	6% (3/54)
Premature Ventricular Contractions / 24 Hr	
N	44
Median	2006.2
Q1 – Q3	514.89 – 3449.96

O 8. Vectorcardiography predictors for poor Fontan outcomes: QRSvm and SPQRS-T angle as noninvasive markers of Fontan failure risk

Ashley Wong¹, Daniel Cortez¹

¹ UC Davis Medical Center, CA, USA

Background: Limited noninvasive methods exist for predicting Fontan failure (FF).

Objective: We demonstrate the use of vectorcardiography (VCG) parameters as a measure of FF risk.

Methods: Fontan patients (completed Fontan after 1990) without ventricular pacing (n=107, age at follow up after Fontan 11 years (IQR 9), women 36.4%) were compared between FF and Fontan survival (FS) groups. FF was defined as protein-losing-enteropathy (PLE), plastic bronchitis(PB), Fontan takedown, transplant, death, or New York Heart Association(NYHA) class III-IV. Analysis included 12-lead ECG/VCG data utilized at last follow up or prior to FF for assessing: PR interval(PR), QRS duration(QRSd), corrected QT-interval(QTc), left sided measures of P-wave, QRS and T-wave vector magnitudes, spatial P-R and QRS-T angles, and right precordial measures of P-wave, QRS, and T-wave vector magnitudes and Right P-R and precordial-directed angles. Cox regression analysis, ROC analysis and Kaplan-Meier survival analysis performed.

Results: 14 patients had FF (13.1%) of which 1.9% PLE, 2.8% PB, 1.9% Fontan takedown, 2.8% NYHA class III-IV, 5.6% heart transplant and 0.9% Death. LV dominance was inversely associated to FF with a p-value of 0.048. HLHS, HR, PR, QTc, Pvm, QRSvm, SPQRST-angle, RtPvm, RtQRSvm and RtTvm were associated with increased hazard ratio (p-value <0.001 to 0.048) for FF. SPQRS-T angle and QRSvm best differentiated FF and FS groups with significantly increased total mortality for QRSvm >1.91 mV and SPQRS-T angle >92.3 deg with p-values of 0.002.

Conclusion: Elevated QRSvm >1.91 mV and widened SPQRS-T angle >92.3 deg obtained from a standard 12-lead ECG can be predictors of FF.

O 9. Electrocardiogram proarrhythmic changes in pregnancy in women with congenital heart disease

Frida Wedlund¹, Constance Weissman¹, Thuva Lindblad¹, Emma von Wowern², Joanna Hlebowicz¹

¹ Department of Cardiology Skåne University Hospital, Lund University, Sweden, ² Department of Obstetrics and Gynecology, Skåne University Hospital, Lund University, Sweden

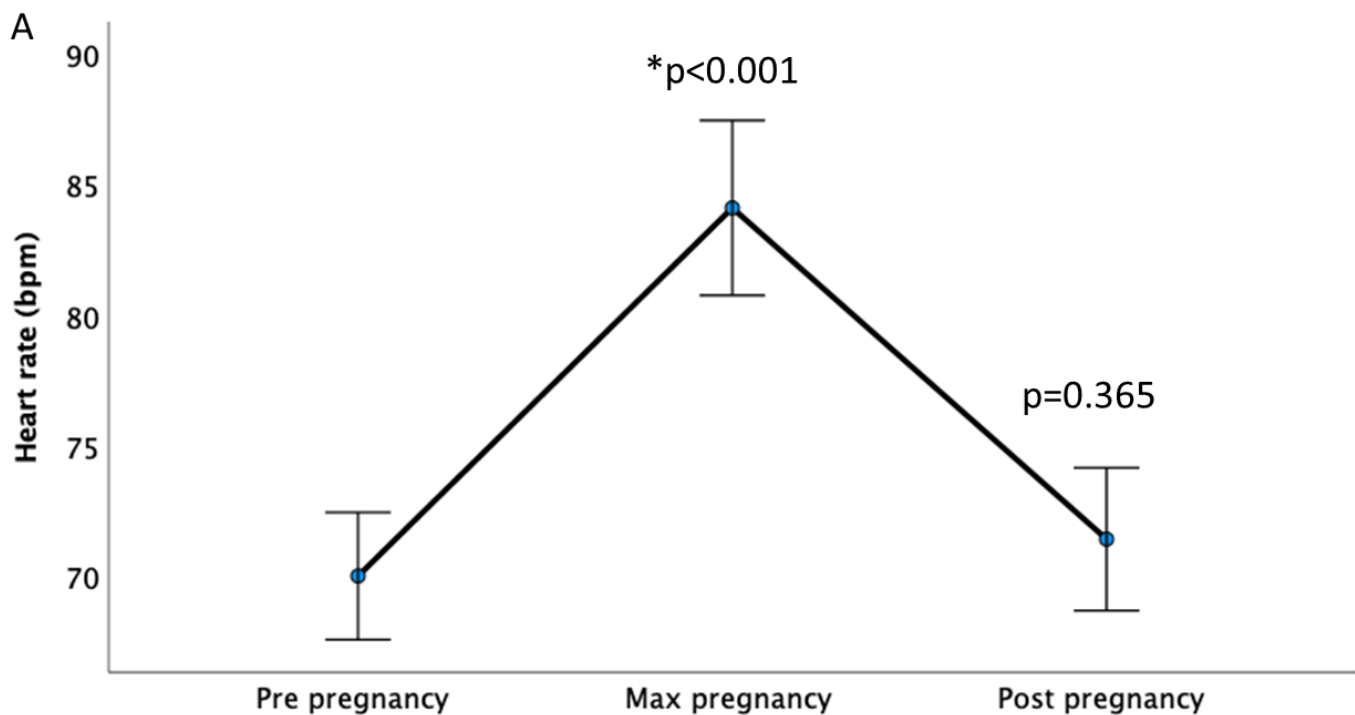
Background: Pregnancy-related physiological adaptations can lead to heart failure or rhythm disturbances, especially in women with cardiac disease. Even in healthy women, physiological adaptations are increased heart rate and electrocardiogram (ECG) changes; shortening of the PR-interval and mean QTc-prolongation of 27 ms.

Purpose: to evaluate ECG differences in congenital heart disease (CHD) women before, during and after pregnancy and to identify risk factors for prolonged QTc-interval, a major risk factor for ventricular arrhythmias.

Methods: ECG-changes during pregnancy were analyzed using t-test for paired samples. Logistic regression was used to analyze risk factors for arrhythmias and risk factors for pre-pregnancy QTc-prolongation >460 ms. Risk factors for QTc-prolongation >460 ms and QTc-increase during pregnancy >27 ms were analyzed using t-test for independent samples (metric data) and chi²-test (categorical data). Risk factors with p<0.1 were further analyzed using logistic regression. P<0.05 was considered statistically significant.

Results: 83 women were included, 15 (18.1%) in mWHO class I, 26 (31.3%) in mWHO II, 28 (33.7%) in mWHO II-III, 11 (13.3%) in mWHO III and three women (3.6%) in mWHO class IV. Three women had documented arrhythmias during pregnancy. Heart rate (p<0.001) and QTc-interval (p=0.001) increased during pregnancy (Figure 1). No difference in QRS-duration or PR-interval was observed (p>0.5). QTc-duration of >460 ms was associated with increased pre-pregnancy QTc-interval, QRS-duration (both p<0.001), weight and body mass index (BMI) (both p=0.03). QTc-increase >27ms was associated with increased heart rate prior to pregnancy (p<0.001). No significant ECG-changes were identified in relation to mWHO class.

Conclusion: ECG-changes in CHD women may differ from previous studies in healthy women. Women with long QRS-duration or long QTc-interval, high weight and/or BMI or high heart rate prior to pregnancy may need to be monitored closely for arrhythmias during pregnancy.



Whole heart modeling

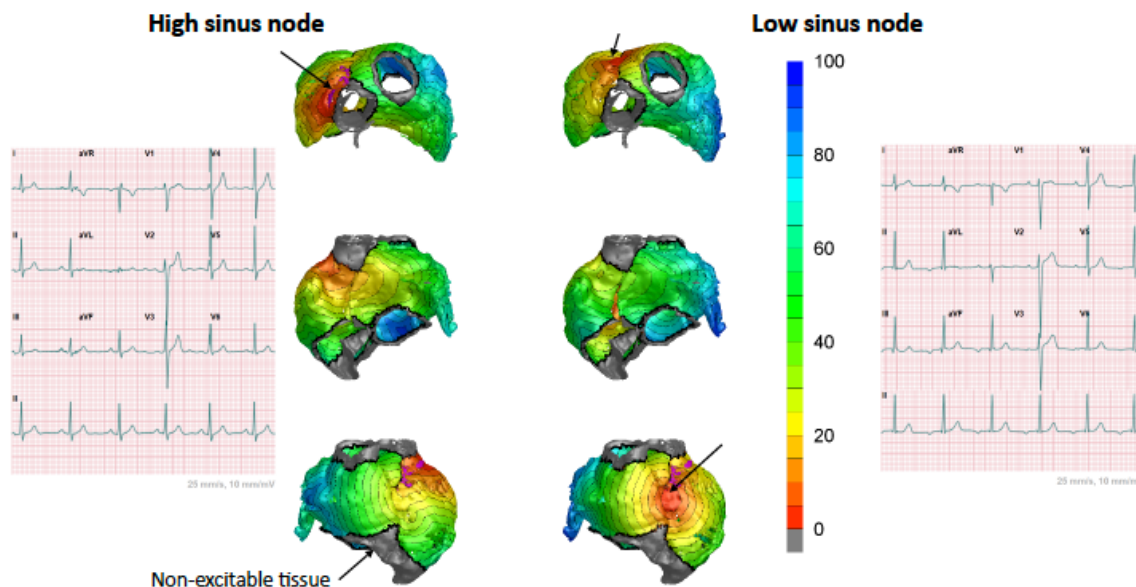
O 10. Atrial anatomy enhanced by mixed reality and 3D representation of ECG generation

Danila Potyagaylo¹, Peter van Dam¹, Klaudia Proniewska¹

¹Center for Digital Medicine and Robotics, Jagiellonian University Medical College, Krakow, Poland
Background: A comprehensive perception of the atria at various levels – histological, electrical, and anatomical - is the target for scientific and teaching efforts among clinicians and academic instructors. Furthermore, the importance of 3D visualization of the cardiac structures and their relation to the ECG genesis is becoming increasingly recognized in assessing patient's functional status. The study of P-wave morphology is also gaining interest due its potential in predicting atrial fibrillation
Methods: The characteristics of the P-wave are influenced by multiple factors, including the sinus node location and extent, exit point in the myocardium starting the sinus rhythm, fast conductive tissue architecture and other physical characteristics of the atrial chambers. We performed Eikonal-based propagation simulations on a highly detailed anatomical atrial model, forwardly computed the respective ECG signals for various sinoatrial node (exit point) locations and qualitatively evaluated the resulting P waves morphologies. Both, atrial anatomy and excitation wave propagation, were exported into the mixed reality Hololens® system for enhanced visualization.

Results: In agreement with the reported findings, P-wave morphology was shown to be highly dependent on the sinus node location. In an interactive manner, we could show that its inferior placement might cause a downward or even negative deflection in the P-wave due to the altered direction of the impulse. A posteriorly located sinoatrial node can make the P-wave more pronounced in the posterior ECG leads.

Conclusions: This work presents novel mixed reality 3D visualization options for atrial anatomy in high spatial resolution augmented by the respective P wave genesis.



Atrial Myopathy

O 11. Interatrial block and atrial fibrillation in ST-elevation myocardial infarction.

Maria Baturova¹, Marina Demidova¹, David Erlinge¹, Pyotr Platonov¹

¹ Department of Cardiology, Clinical Sciences, Lund University, Sweden

Background: Interatrial blocks (IAB) reflect atrial abnormalities contributing to atrial fibrillation (AF). New onset AF (newAF) is a known complication during acute ST-segment elevation myocardial infarction (STEMI). Whether IAB associated with AF in population-based studies can predict ischemia-triggered AF is not fully clarified.

Purpose: To assess the association of IAB with newAF during acute STEMI and long-term follow-up.

Methods: Study sample comprised of STEMI patients admitted for primary percutaneous intervention from 2007 to 2010 (n=1472, age 68 years, 33% females). Clinical information was collected from the SWEDEHEART registry. The closest sinus rhythm ECGs prior to STEMI (time ECG-to-STEMI 1.2 [IQR 0.3-3.8] years), were extracted from the digital ECG database and processed using Glasgow algorithm. IAB was defined as a P-wave ≥ 120 ms and classified as partial (positive P-wave in three inferior leads or biphasic P-wave in III only [pIAB]) or advanced IAB (biphasic P-wave in III and aVF or all three inferior leads [aIAB]).

Results: After exclusion of 75 patients (5%) with pre-existing AF, 1397 patients were included in analysis. Pre-existing pIAB was observed in 402 (29%) patients and aIAB in 68 (5%). NewAF was observed in 108 patients (7%). In logistic regression analysis adjusted for age IAB was not associated with newAF (OR for pIAB 1.47 95% CI 0.95-2.29, for aIAB 2.03 95% CI 0.96-4.29). During follow-up, incident AF was documented in 206 (16%) of 1289 patients discharge alive without AF during hospital stay. In the multivariate Cox regression analysis aIAB was independently associated with incident AF (HR 2.80 95% CI 1.41-5.55, Figure).

Conclusion: Atrial conduction abnormalities are associated with increased risk of incident AF after discharge from STEMI but are not predictive of ischemia-triggered AF, suggesting different mechanisms behind AF in the ischemic and non-ischemic settings.

Kaplan-Meier Survival Curve

